ACADEMIC PRESS

Available online at www.sciencedirect.com

SCIENCE DIRECT®

Journal of Sound and Vibration 268 (2003) 1–14

JOURNAL OF SOUND AND VIBRATION

www.elsevier.com/locate/jsvi

In-plane antisymmetric response of cables through bifurcation under symmetric sinusoidally time-varying load

K. Takahashi*, Q. Wu, S. Nakamura

Department of Civil Engineering, Faculty of Engineering, Nagasaki University, 1-14 Bunkyo-machi, Nagasaki 852-8521, Japan

Received 20 May 2002; accepted 4 November 2002

Abstract

Analysis and results for in-plane non-linear antisymmetric responses of a cable, supported at the same level, through bifurcation under in-plane symmetric sinusoidally time-varying load are presented. The non-linear equation of the in-plane motion of the cable is solved by a Galerkin method and the harmonic balance method. From the computed results the frequency range, where the antisymmetric response occurs, varies with the sag-to-span ratio of the cable and is broad in the particular sag-to-span ratios. The second unstable region is important compared with the principal unstable region. Strong coupling between symmetric and antisymmetric modes is observed in the unstable regions for the particular sag-to-span ratios.

1. Introduction

Non-linear vibrations of sagged cables have been treated by many authors as the dynamic properties of the cable could only be established by considering large deflections. Recently, non-linear vibrations of the sagged cables have been reported by many authors (see references of papers [1,2], and new references [3–7]). Out-of-plane responses bifurcate under in-plane forcing in the particular frequency range [2] and there is a strong interaction between the in-plane and out-plane vibrations.

It was observed in a wind tunnel test that the mode of vibration of a transmission cable is either symmetric or antisymmetric dependent upon wind velocity [8]. This phenomenon is assumed to arise from the dynamic stability of the cable as well as self-excited force. A similar problem was

*Corresponding author.
E-mail address: takahasi@civil.nagasaki-u.ac.jp (K. Takahashi).

0022-460X/03/$ - see front matter
doi:10.1016/S0022-460X(02)01492-X

observed in beam vibration. The antisymmetric responses of the straight beam under symmetric sinusoidally time-varying load are reported by Bennett and Eisley [9] and Takahashi [10]. Since the cable has sag [1,11], the quadratic and cubic non-linear terms are simultaneously included in the equation of motion of the cable. It is expected that the antisymmetric response of a cable is more important than that of a straight beam.

The present work considers in-plane non-linear antisymmetric responses of horizontal cables under an in-plane symmetric sinusoidally time-varying load. The method of solution is roughly the same as that in [1,2]. The various possible types of solution are obtained with techniques of the non-linear oscillation theory. The non-linear equation of in-plane motion is solved by a Galerkin method in space co-ordinates. The frequency range where the antisymmetric responses exist is obtained and presented for various sag-to-span ratios by the linear theory of the antisymmetric responses. Coupling between symmetric and antisymmetric modes having periodic solutions at the unstable boundaries is obtained by the harmonic balance method. Those having non-periodic solutions within unstable regions are obtained by using the Runge–Kutta–Gill method.

2. Method of solution

A horizontal cable with uniform cross-section hanging between two fixed points, as shown in Fig. 1, is considered. If the profile is flat, so that the sag-to-span ratio is 1:8 or less, the equations of motion of the non-linear vibrations of a cable subjected to in-plane vertical symmetric time-varying load are obtained as follows [11]:

$$m\frac{\partial^2 w}{\partial t^2} - (H + \Delta H)\frac{\partial^2 w}{\partial x^2} + \Delta H\frac{8f}{L^2} = p_0 \cos \Omega t, \tag{1}$$

$$\Delta H = \frac{EA}{L_E}\left\{\frac{mg}{H}\int_0^L w\,\mathrm{d}x + \frac{1}{2}\int_0^L \left(\frac{\partial w}{\partial x}\right)^2 \mathrm{d}x\right\}, \tag{2}$$

where w is the vertical displacement, x is the span-wise co-ordinate , t is time, H is the horizontal component of the cable tension, ΔH is the deflection-induced additional tension, m is the mass per unit length of the cable, g is the acceleration due to gravity, E is the modulus of elasticity of the cable, A is the cross-sectional area, $L_E = L\{1 + 8(f/L)^2\}$ is the length of the cable, L is the span of the cable, f is the sag of the cable, Ω is the radian frequency of the vertical load, and p_0 is the uniformly distributed vertical load intensity.

If we assume the present problem to be a two-degree-of-freedom dynamic system, which is composed of the symmetric mode and the antisymmetric mode, a normal mode of solution is

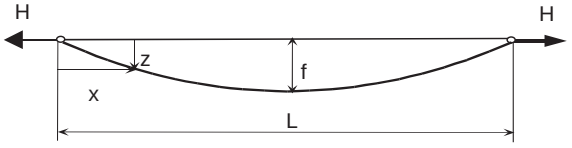

Fig. 1. Geometry of a cable.

assumed as [1]

$$\bar{w}(\bar{x},\tau) = L\sum_{i=1}^{2} P_i(\tau)W_i(\bar{x}), \tag{3}$$

where $P_i(\tau)$ is a known function of time which is a generalized co-ordinate of response, $W_i(\bar{x})$ is the space co-ordinate function satisfying the associated linear problem (W_i is zero at both ends), and as obtained by linear free vibration analysis is given by [11]

$$\begin{aligned} W_1(\bar{x}) &= 1 - \tan\frac{\bar{\omega}_1\pi}{2}\sin\bar{\omega}_1\pi\bar{x} - \cos\bar{\omega}_1\pi\bar{x}, \\ W_2(\bar{x}) &= \sin(\bar{\omega}_2\pi\bar{x}). \end{aligned} \tag{4}$$

Here $\bar{x} = x/L$ is the non-dimensional co-ordinate in the x direction, $\tau = \omega_0 t$ is the non-dimensional time, $\omega_0 = [(H/m)(\pi/L)^2]^{1/2}$ is the first natural circular frequency of the taut string which has no sag, $\bar{\omega}_i = \omega_i/\omega_0$ is the non-dimensional natural circular frequency, $\bar{\omega}_2 = 2$ is the non-dimensional natural circular frequency of the antisymmetric mode and $\bar{\omega}_1$ is the non-dimensional natural circular frequency of the symmetric mode obtained by the following equation:

$$\tan\frac{\bar{\omega}_1\pi}{2} = \frac{\bar{\omega}_1\pi}{2} - \frac{4}{\lambda^2}\left(\frac{\bar{\omega}_1\pi}{2}\right)^3, \tag{5}$$

where $\lambda^2 = 64k^2\gamma^2/(1+8\gamma^2)$ is the Irvine parameter [11], $k^2 = EA/H$ is the ratio of elongation stiffness to horizontal tension of the cable and $\gamma = f/L$ is the sag-to-span ratio of the cable.

Applying a Galerkin method to Eqs. (1) and (2), one has the following ordinary differential equations for the time variables:

$$\ddot{P}_1(\tau) + a_1P_1 + b_1P_1^2 + c_1P_2^2 + d_1P_1^3 + e_1P_1P_2^2 = f_1\bar{p}\cos\bar{\omega}\tau, \tag{6}$$

$$\ddot{P}_2(\tau) + a_2P_2 + \left(b_2P_1 + c_2P_1^2 + d_2P_2^2\right)P_2 = 0, \tag{7}$$

where a_1-f_1 and a_2-d_2 are coefficients dependent on the modal shapes of the linear problem (see Appendix A) and $\bar{p} = p_0/mg$.

3. Classifications of solutions

Eq. (7) is a homogeneous equation satisfied by $P_2 = 0$. Then, Eq. (6) reduces to just the function P_1. The non-linear symmetric response of the accompanying type (P_1), that is, the non-linear symmetric response subjected to the symmetric sinusiodally time-varying load can be obtained by using the following equation:

$$\ddot{P}_1(\tau) + a_1P_1 + b_1P_1^2 + d_1P_1^3 = f_1\bar{p}\cos\bar{\omega}\tau. \tag{8}$$

On the other hand, since the symmetric time function P_1 is included as coefficients in Eq. (7) as can be seen in Eq. (7), the antisymmetric time function of P_2 may be obtained through bifurcation. The non-linear symmetric response occurs near $\bar{\omega} = \bar{\omega}_1$ and the non-linear antisymmetric response through bifurcation occurs near the second unstable region $\bar{\omega} = \bar{\omega}_2$ and

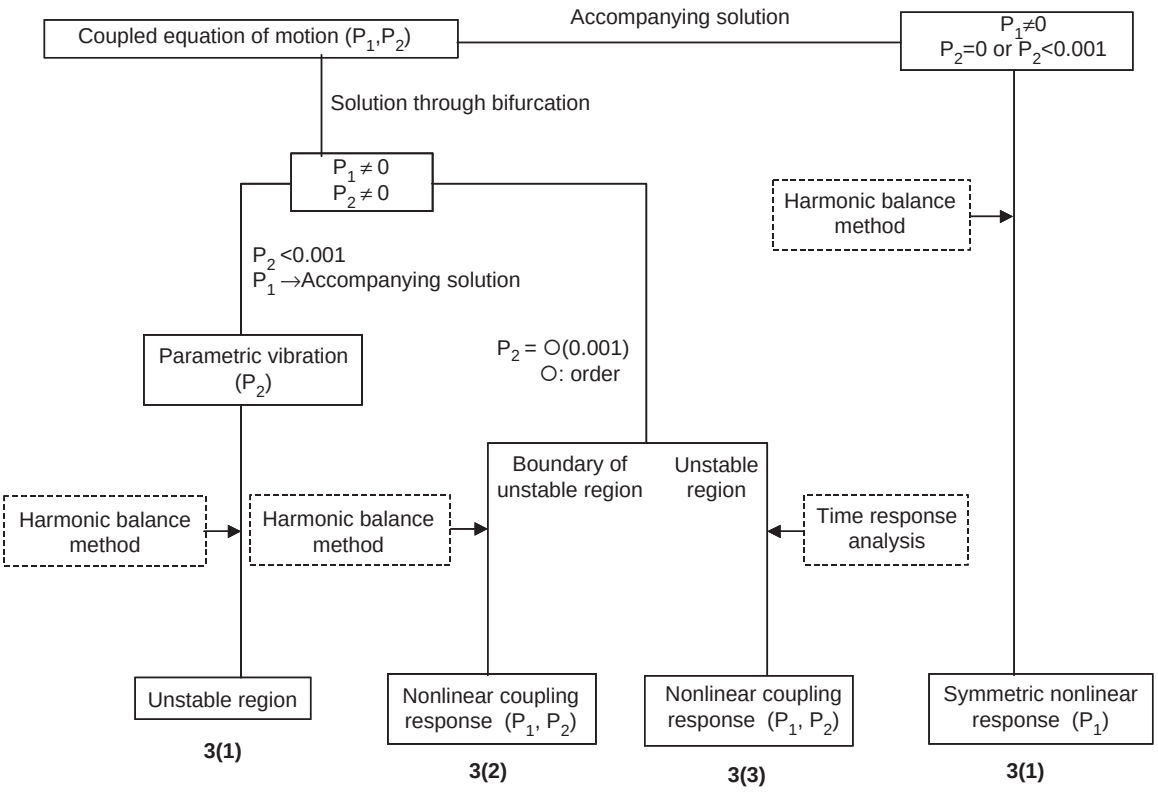

Fig. 2. Classifications of the solution and its approach.

the principal unstable region $2\bar{\omega}_2$. If non-linear quadratic and cubic terms P_2^2 and P_2^3 are neglected, a parametric antisymmetric response can be obtained by using the theory of dynamic stability to identify the unstable regions [10]. A symmetric response can be obtained independently by using Eq. (8). Non-linear quadratic and cubic terms, P_2^2 and P_2^3, cannot be neglected in the case of large amplitude vibrations; coupling non-linear responses between $P_1$and P_2 are obtained from Eqs. (6) and (7). Coupling non-linear responses near bifurcation points should be obtained by using the harmonic balance method and those within the unstable regions can be obtained by a time response analysis. From these considerations, classification of the solution to this problem is shown in Fig. 2.

3.1. Unstable regions of parametric vibration

If we obtain a solution in the neighborhood of the bifurcation point, the non-linear term as to P_2^2 can be neglected. Then, Eqs. (6) and (7) can be rewritten as follows:

$$\ddot{P}_1 + a_1 P_1 + b_1 P_1^2 + d_1 P_1^3 = f_1 \bar{p} \cos \bar{\omega}\tau, \tag{9}$$

$$\ddot{P}_2 + a_2 P_2 + \left(b_2 P_1 + c_2 P_1^2\right) P_2 = 0. \tag{10}$$

Eq. (9) is a function of P_1 only and then can be solved independently when P_1 is assumed as

$$P_1 = \tfrac{1}{2}C_0^1 + C_1^1 \cos\bar{\omega}\tau, \tag{11}$$

where C_0^1 and C_1^1 are amplitude components.

By using these amplitude components of the symmetric responses C_0^1 and C_1^1 obtained from Eq. (9), Eq. (10) is reduced to the Hill equation as

$$\ddot{P}_2 + a_2 P_2 + (D_1 + D_2 \cos\bar{\omega}\tau + D_3 \cos 2\bar{\omega}\tau)P_2 = 0, \tag{12}$$

where $D_1 = a_2 + \frac{1}{2}b_2 C_0^1 + \frac{1}{4}c_2 C_0^1 C_0^1 + \frac{1}{2}c_2 C_1^1 C_1^1$, $D_2 = b_2 C_1^1 + c_2 C_0^1 C_0^1$, $D_3 = \frac{1}{2}c_2 C_1^1 C_1^1$.

The solution of Eq. (12) is assumed as follows [10]:

$$P_2 = \mathrm{e}^{\lambda\tau}\left\{\frac{1}{2}\beta_0 + \sum \alpha_n \sin(n\bar{\omega}\tau) + \beta_n \cos(n\bar{\omega}\tau)\right\}, \tag{13}$$

where λ is an unknown constant, and β_0, β_n and α_n are unknown coefficients.

Substituting Eq. (13) into Eq. (12), a homogeneous equation to seek for λ is obtained. The stability of this equation is evaluated by using the method shown in Ref. [10].

3.2. Non-linear coupling responses on the unstable boundary

Non-linear antisymmetric response occurs near the frequency $\bar{\omega} = 2\bar{\omega}_2 = 2.0$ (boundaries of the principal unstable region with period $2T = 4\pi/\bar{\omega}_2$) and $\bar{\omega} = \bar{\omega}_2 = 2.0$ (boundaries of the second unstable region with period $2\pi/\bar{\omega}_2$). From the above consideration, a solution of Eqs. (6) and (7) is assumed as

$$P_1 = \tfrac{1}{2}C_0^1 + C_1^1 \cos\bar{\omega}\tau, \tag{14}$$

$$P_2 = \tfrac{1}{2}C_0^2 + C_{1/2}^2 \cos\frac{\bar{\omega}\tau}{2} + S_{1/2}^2 \sin\frac{\bar{\omega}\tau}{2} + C_1^2 \cos\bar{\omega}\tau + S_1^2 \sin\bar{\omega}\tau, \tag{15}$$

where C_0^2, $C_{1/2}^2$, $S_{1/2}^2$, C_1^2 and S_1^2 are the amplitude components of the antisymmetric time function.

Substituting Eqs. (14) and (15) into Eqs. (6) and (7) and applying the harmonic balance method yield a set of non-linear algebraic relations for determining the unknown constants. The non-linear equations may be solved by the Newton–Raphson method with the use of a proper initial guess.

In the practical numerical calculation, putting the amplitude components ($C_0^2 \sim S_1^2$) at zero and obtaining the symmetric components, C_0^1 and C_1^1, the frequency–response curve of the symmetric vibration can be obtained. Then amplitude components of the antisymmetric responses near $\bar{\omega} = 2\bar{\omega}_2$ and $\bar{\omega} = \bar{\omega}_2$ are obtained by assuming non-zero initial values of the amplitude components.

3.3. Non-linear coupling response within unstable regions

It is impossible to obtain a solution to Eqs. (6) and (7) within an unstable region. Time variables P_1 and P_2 can be numerically integrated. The Runge–Kutta–Gill method is used in the present analysis to determine the amplitudes of unstable motions. The initial conditions for the time variable P_1 are $P_1(0) = a$ steady state response under a symmetric load, $\dot{P}_1(0) = 0.0$. The initial condition for the time variable P_2 are $P_2(0) = 0.0$ and $\dot{P}_1(0) = 0.001$.

4. Basic properties of coupling response

The natural frequency $\bar{\omega}_1$ of the symmetric mode and the natural frequency $\bar{\omega}_2$ of the antisymmetric mode of a cable with $k = 30$ are shown in Fig. 3. The antisymmetric mode is not affected by the sag-to-span ratio γ ($\bar{\omega}_2 = 2.0$). On the other hand, the effect of the sag-to-span ratio is considerable on the symmetric mode; that is, a modal crossover occurs from the first symmetric mode to the next one in the particular sag-to-span ratio and the frequency increases ($\bar{\omega}_1 = 1.0 \rightarrow 3.0$) [11]. From this fact, the two natural frequencies have the following relations: $\bar{\omega}_1 < \bar{\omega}_2$ ($\gamma < 0.026$), $\bar{\omega}_1 \approx \bar{\omega}_2$ ($\gamma \approx 0.026$) and $\bar{\omega}_1 > \bar{\omega}_2$ ($\gamma > 0.026$). The exciting force from the symmetric vibration P_1 to the antisymmetric vibration P_2 depends on the exciting terms, $b_2 P_1$ and $c_2 P_1^2$, in Eq. (7). The feedback terms to the symmetric vibration from the antisymmetric vibration are $c_1 P_2^2$ and $e_1 P_2^2 P_1$ in Eq. (6).

The coefficients, c_1 and e_1, are shown as a function of γ in Figs. 4 and 5. These coefficients, c_1 and e_1, change with an increase of γ. They are small when γ is very small and the effect of the antisymmetric vibration on the symmetric vibration is small. The coefficient c_1 increases with an increase of sag-to-span ratio γ, and approaches a maximum value near $\gamma = 0.04$. Then it decreases for greater sag-to-span ratio. The coefficient c_1 is large where the modal crossover is produced. The coefficient e_1 increases near $\gamma = 0.04$ and becomes a maximum near $\gamma = 0.06$.

The parametric exciting coefficients b_2 and c_2 are shown in Figs. 6 and 7 as functions of the sag-to-span ratio γ with results similar to c_1 and e_1. These parametric exciting and feedback coefficients of cables are greater than those of a string whose sag-to-span ratio is small. It is assumed that the strong coupling between the symmetric and the antisymmetric modes under a symmetric sinusoidally time-varying load appears in the cable vibration.

5. Numerical results

5.1. Symmetric and antisymmetric non-linear response curves

The non-linear symmetric responses and corresponding antisymmetric responses are presented for cables with $k = 30$. The non-linear symmetric response occurs near the frequency range

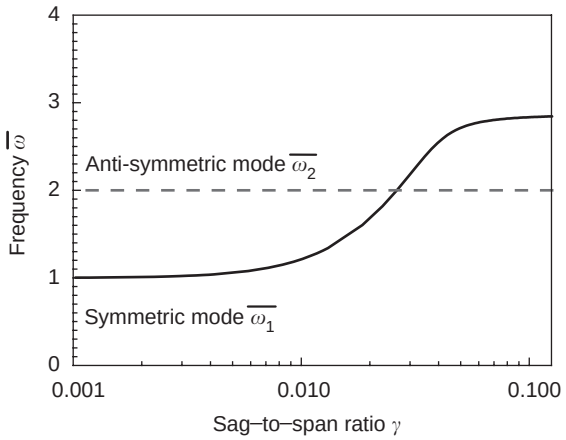

Fig. 3. Relation between the first symmetric frequency $\bar{\omega}_1$ and the first antisymmetric frequency $\bar{\omega}_2$.

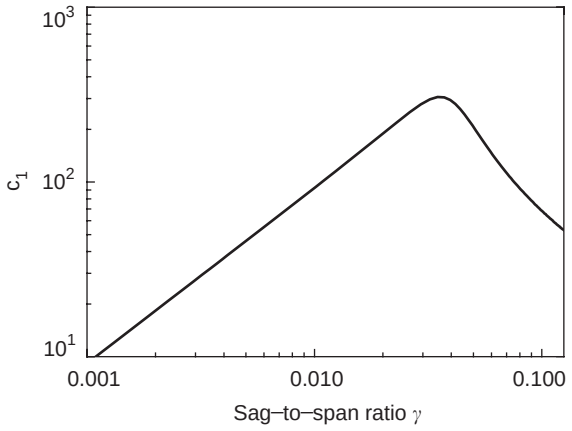

Fig. 4. Relation between feedback term c_1 and sag-to-span ratio γ.

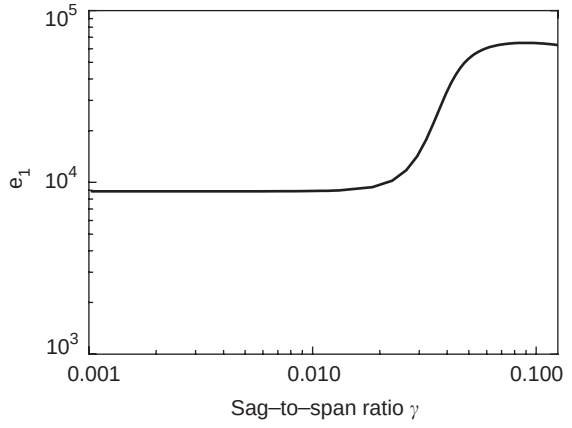

Fig. 5. Relation between feedback term e_1 and sag-to-span ratio γ.

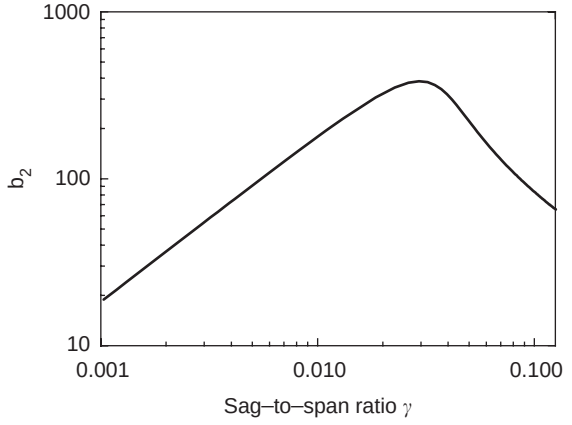

Fig. 6. Relation between parametric exciting term b_2 and sag-to-span ratio γ.

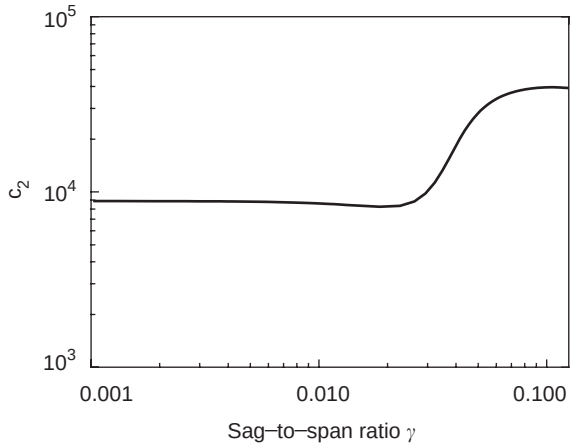

Fig. 7. Relation between parametric exciting term c_2 and sag-to-span ratio γ.

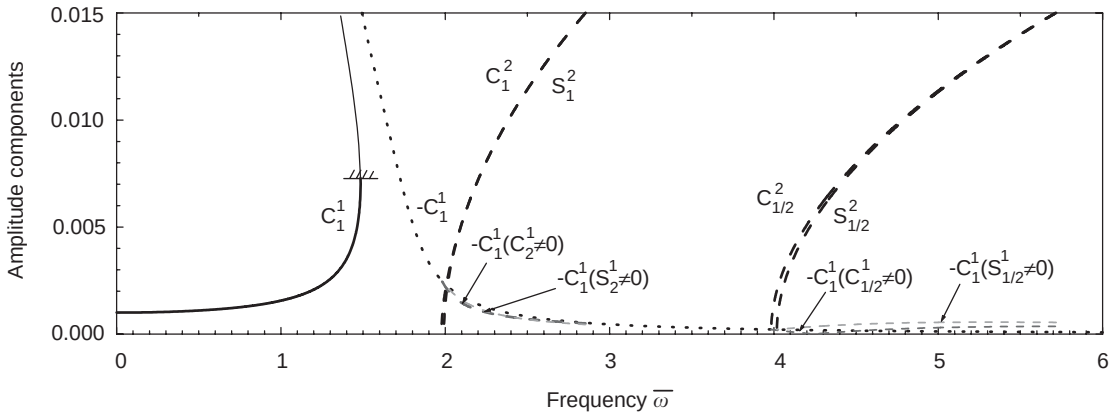

Fig. 8. Symmetric and antisymmetric non-linear responses of a cable with $\gamma = 0.020$ and $\bar{p} = 0.132$.

$\bar{\omega} = \bar{\omega}_1$, while the antisymmetric response occurs near $\bar{\omega} = \bar{\omega}_2$ and $2\bar{\omega}_2$. There are three different types of symmetric and antisymmetric responses at the unstable boundary as shown in Figs. 8–10.The sag-to-span ratios of these figures are γ =0. 02 ($\bar{\omega}_2 > \bar{\omega}_1$), γ =0. 022 ($\bar{\omega}_2 \approx \bar{\omega}_1$) and γ =0.07 ($\bar{\omega}_2 < \bar{\omega}_1$). The load intensity for each case is adjusted so as to give the same static response, 0.001, when $\bar{\omega} = 0$. In these figures, the ordinate indicates the amplitude components (i.e., $C_1^1, S_1^2, C_1^2, S_{1/2}^2, C_{1/2}^2$). The amplitude of the symmetric response (C_1^1) is defined by that of the center of the cable, while the amplitude of the antisymmetric response is defined by that of the quarter point of the cable.

In these figures, the thicker solid lines and dotted lines correspond to the in-phase and out-of-phase symmetric responses, respectively. These symmetric responses exist in the entire frequency range. Symmetric non-linear responses show a softening spring or a hardening spring depending upon the sag-to-span ratio as shown in Figs. 8–10. On the other hand, the thinner dotted lines

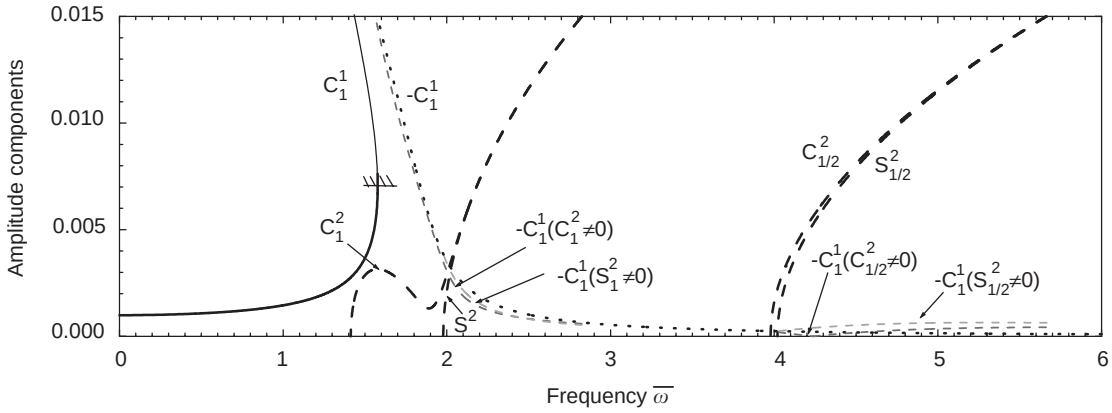

Fig. 9. Symmetric and antisymmetric non-linear responses of a cable with $\gamma = 0.022$ and $\bar{p} = 0.133$.

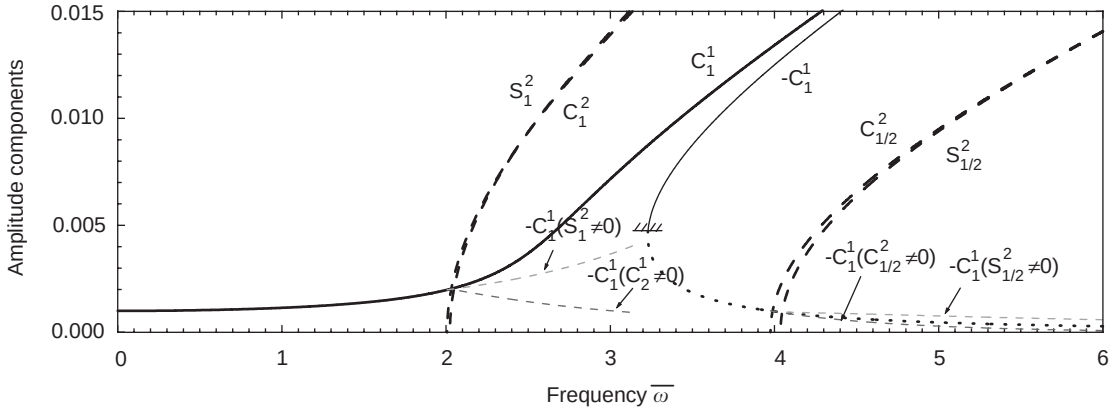

Fig. 10. Symmetric and antisymmetric non-linear responses of a cable with $\gamma = 0.070$ and $\bar{p} = 0.609$.

near $\bar{\omega} = 2\bar{\omega}_2$ and $\bar{\omega}_2$ correspond to the antisymmetric responses at the unstable boundary through bifurcation. The relation between amplitude and frequency of the antisymmetric response curve shows a tendency of the weakly hardening spring independent of the sag-to-span ratio. The amplitude of the symmetric response after the bifurcation is different from that of the symmetric response without the antisymmetric response. The phase angle of the antisymmetric response is either in-phase or out-of-phase and its absolute value is the same.

The antisymmetric responses of the principal and second unstable regions occur from the out-of-phase symmetric response of a cable with a sag-to-span ratio $\gamma = 0.02$, because $\bar{\omega}_2$ is greater than $\bar{\omega}_1$ as shown in Fig. 8. The second unstable motion occurs from the in-phase symmetric response of a cable with a sag-to-span ratio $\gamma = 0.07$ because $\bar{\omega}_2$ is less than $\bar{\omega}_1$ as shown in Fig. 10. Contrary to these, in the case of a cable with $\gamma = 0.022$, the bifurcation point of the second unstable motion near $\bar{\omega} = 2.0$ coincides with the natural frequency $\bar{\omega}_2$ of the symmetric response. Therefore, bifurcation responses S_1^2 and C_1^2 occur from the in-phase and out-of-phase responses of the symmetric vibration, respectively. As the symmetric non-linear response of the cable with $\gamma = 0.022$ shows a softening spring, the symmetric response has a vertical tangent as

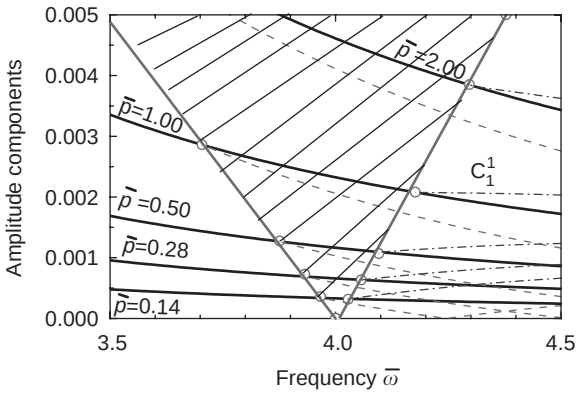

Fig. 11. Principal unstable region of the antisymmetric response of a cable with $\gamma = 0.026$.

shown in Fig. 9. The shaded side of the in-phase response curve is unstable and its amplitude in this range cannot be realized. Therefore, the antisymmetric response which bifurcates from the symmetric response C_1^1 does not exist. In the present case, the frequency range where the antisymmetric response occurs is defined by the vertical tangent of the out-of-phase symmetric response.

The principal unstable response occurs in the frequency range of $2\bar{\omega}_2$ and the frequency $2\bar{\omega}_2$ is greater than $\bar{\omega}_1$ independent of the sag-to-span ratio γ. The principal unstable response always occurs from the out-of-phase symmetric response.

The principal unstable region near $2\bar{\omega}_2$ of the cable with $\gamma = 0.026$ is shown in Fig. 11 for various load intensities. The result is obtained by linear analysis as shown in Section 3.1. The shaded area is the unstable region where the antisymmetric response diverges. The boundary curves separating the stable regions from the unstable regions have periodic solutions with a period 2 T. These boundaries coincide with bifurcation points obtained by the non-linear analysis as shown in Section 3.2. The width of the unstable region grows wider as the load intensity increases as shown in Fig. 11.

5.2. Principal and second unstable regions

Figs. 12 and 13 show frequency ranges of the principal and second unstable regions of a cable ($k = 30$) as functions of the sag-to-span ratio γ by adjusting load intensity to give the same static response. The load intensity $\bar{p}$ is the triple times used in Figs. 8–10.

The principal unstable region is obviously wider in the range of the sag-to-span ratio $\gamma > 0.01$ than the other sag-to-span ratios. Therefore, the antisymmetric response with a period 2 T occurs for cables with $\gamma > 0.01$.

The second unstable region near $\bar{\omega} = \bar{\omega}_2$ is discontinuous where the sag-to-span ratio $\gamma = 0.02 \sim 0.03$. It is interesting as it is an uncommon result that the second unstable region is wider than the principal unstable region.

These unstable regions of the antisymmetric response are characteristic of the cable. Their extension is narrow when the sag-to-span ratio is small and the antisymmetric response cannot

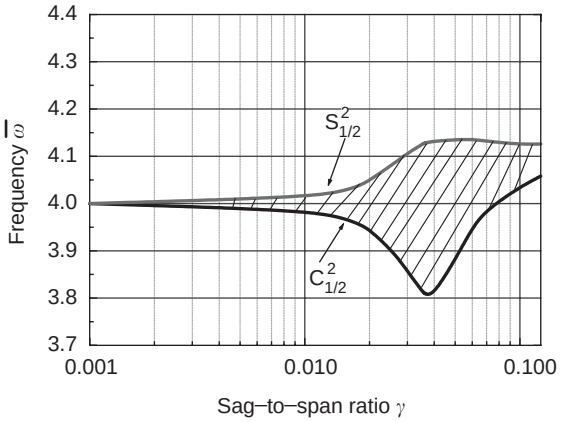

Fig. 12. Principal unstable region of the antisymmetric mode.

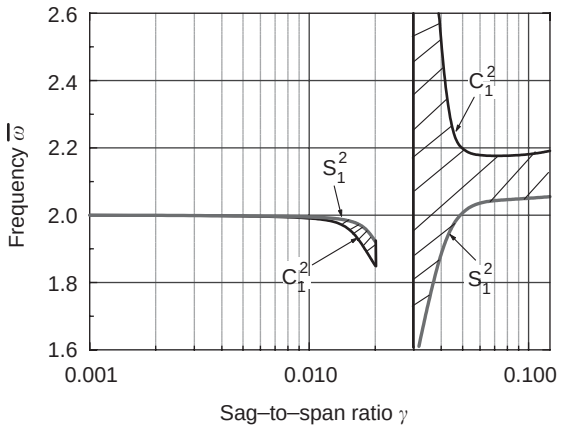

Fig. 13. Second unstable region of the antisymmetric mode.

appear when damping is considered. From these results, a non-linear antisymmetric response occurs in the particular frequency range under symmetric forcing in the case of a horizontal cable.

5.3. Non-linear coupling in unstable regions

Figs. 14 and 15 show time histories of the principal and second unstable regions ($\bar{\omega} = 3.97$ and 2.00) of a cable with $\gamma = 0.03$. A strong non-linear coupling between symmetric and antisymmetric modes can be seen in the time histories. The antisymmetric response influences the symmetric response. Amplitudes of coupling in the second unstable region are greater than those in the principal unstable regions.

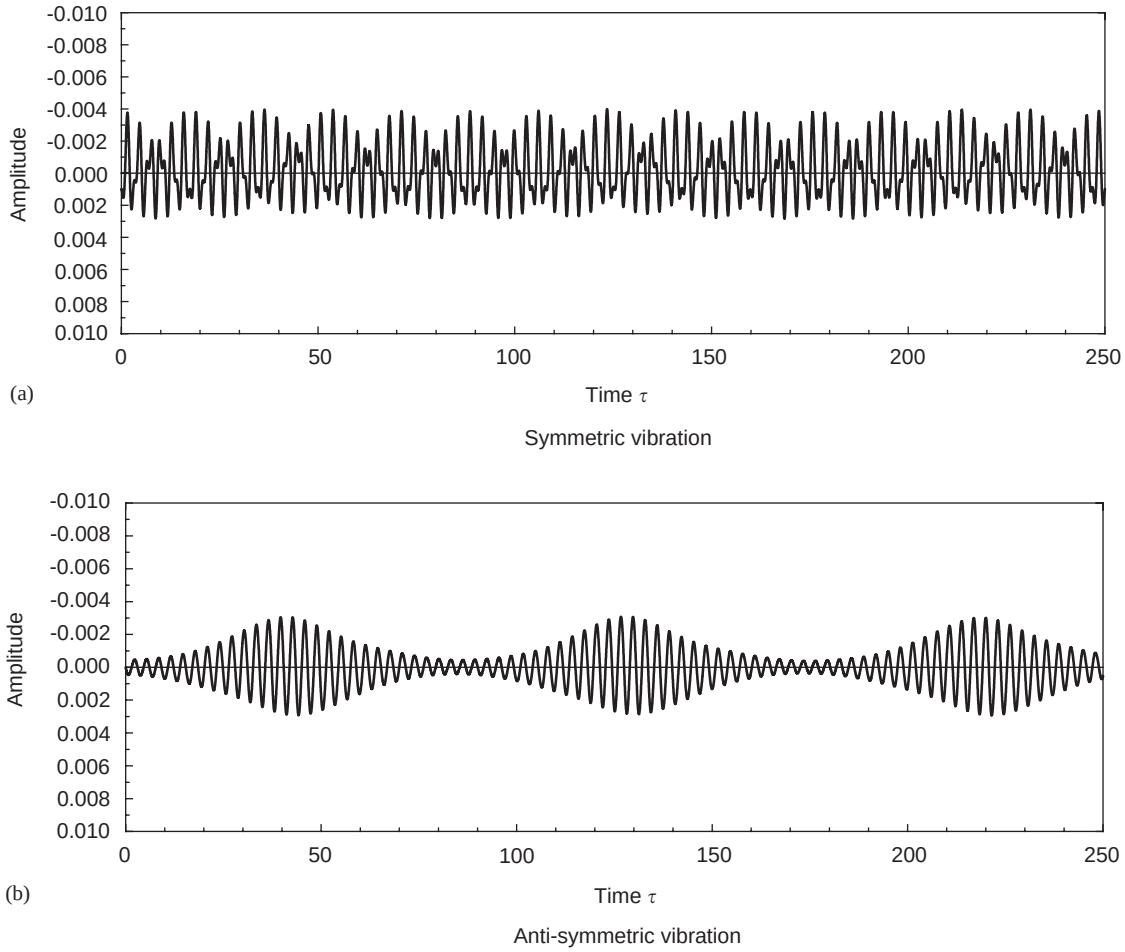

Fig. 14. Time history of a cable within the principal unstable region: $\gamma = 0.03$, $\bar{p} = 0.444$ and $\bar{\omega} = 3.97$.

From these considerations, it is concluded that coupling between the symmetric and antisymmetric modes is observed in a cable under a symmetric load.

6. Conclusions

In the present paper, the non-linear antisymmetric response of a symmetrically supported cable at the same level is presented. Conclusions are as follows:

(1) The antisymmetric response of a cable occurs through bifurcation. The frequency range where the antisymmetric response occurs depends on the sag-to-span ratio of the cable. The uncommon result that the width of the second unstable region is greater than that of the principal unstable region occurs in the cable vibration.

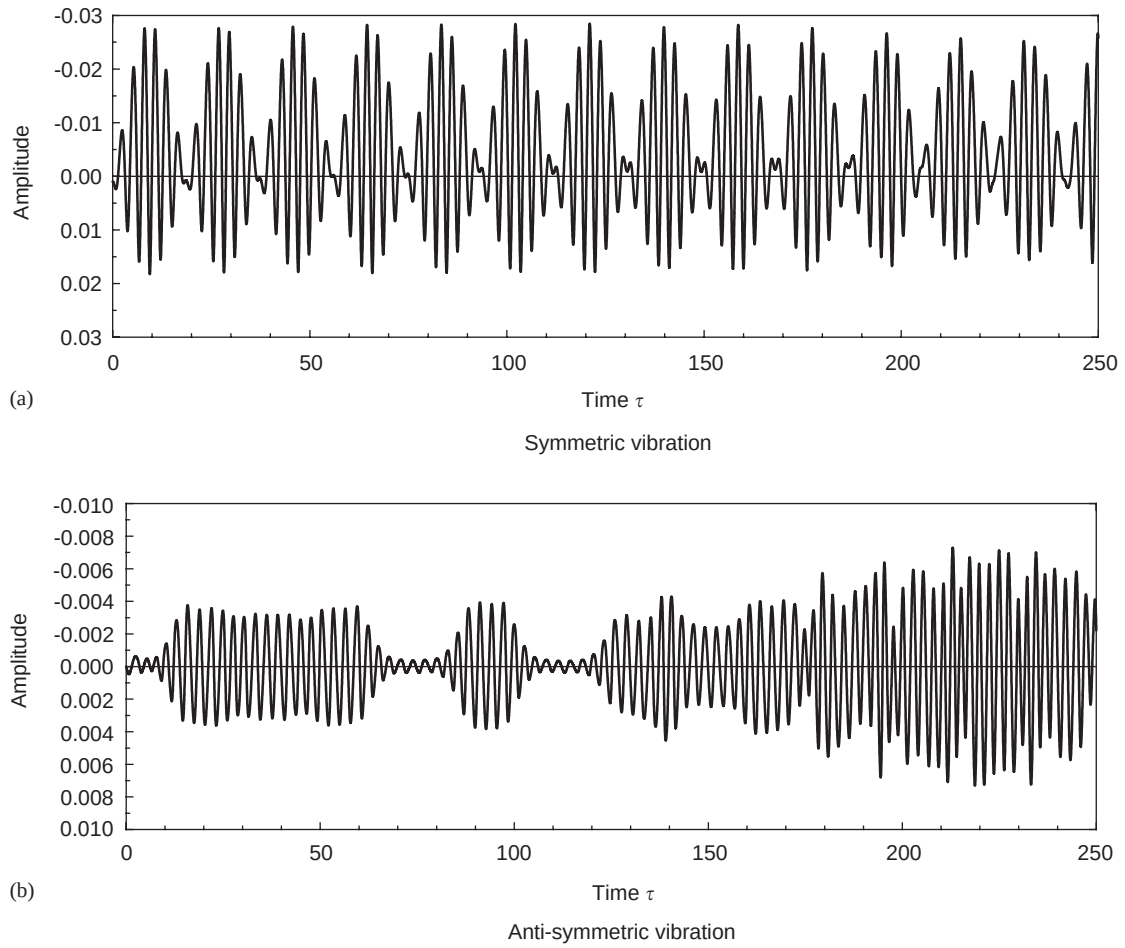

Fig. 15. Time history of a cable within the second unstable region: $\gamma = 0.03$, $\bar{p} = 0.444$ and $\bar{\omega} = 2.00$.

(2) Strong coupling between symmetric and antisymmetric responses is observed within the unstable regions at the sag-to-span ratios studied.

Appendix A. Coefficients of Eqs. (6) and (7)

$$a_1 = \frac{1}{M_1}\left\{-\frac{1}{\pi^2}B_1^1 + \frac{\lambda^2}{\pi^2}K_1K_1\right\}, \quad b_1 = \frac{1}{M_1}\frac{1}{\gamma}\left(-\frac{\lambda^2}{8\pi^2}K_1B_1^1 - \frac{\lambda^2}{16\pi^2}K_1B_1^1\right),$$

$$c_1 = \frac{1}{M_1}\frac{1}{\gamma}\left\{-\frac{\lambda^2}{16\pi^2}K_1B_2^2\right\},$$

$$d_1 = \frac{1}{M_1}\frac{1}{\gamma^2}\left\{\frac{\lambda^2}{128\pi^2}B_1^1B_1^1\right\}, \quad e_1 = \frac{1}{M_1}\frac{1}{\gamma^2}\left\{\frac{\lambda^2}{128\pi^2}B_2^2B_1^1\right\}, \quad f_1 = \frac{1}{M_1}\gamma\left\{-\frac{8}{\pi^2}K_1\right\},$$

$$a_2 = \frac{1}{M_2}\left\{-\frac{1}{\pi^2}B_2^2\right\} = 4, \quad b_2 = \frac{1}{M_2}\frac{1}{\gamma}\left\{-\frac{\lambda^2}{8\pi^2}K_1 B_2^2\right\}, \quad c_2 = \frac{1}{M_2}\frac{1}{\gamma^2}\left\{\frac{\lambda^2}{128\pi^2}B_1^1 B_2^2\right\},$$

$$d_2 = \frac{1}{M_2}\frac{1}{\gamma^2}\left\{\frac{\lambda^2}{128\pi^2}B_2^2 B_2^2\right\}.$$

where

$$M_1 = \int_0^1 W_1^2(\bar{x})\,\mathrm{d}\bar{x}, \quad M_2 = \int_0^1 \sin^2(2\pi\bar{x})\,\mathrm{d}\bar{x} = \tfrac{1}{2}, \quad K_1 = \int_0^1 W_1(\bar{x})\,\mathrm{d}\bar{x},$$

$$B_1^1 = \int_0^1 (\mathrm{d}^2 W_1(\bar{x})/\mathrm{d}^2\bar{x})W_1(\bar{x})\,\mathrm{d}\bar{x}, \quad B_1^1 = \int_0^1 (\mathrm{d}^2 W_1(\bar{x})/\mathrm{d}^2\bar{x})W_1(\bar{x})\,\mathrm{d}\bar{x},$$

$$B_2^2 = \int_0^1 (-4\pi^2)\sin^2(2\pi\bar{x})\mathrm{d}\bar{x} = -2\pi^2.$$

References

[1] K. Takahashi, Y. Konishi, Nonlinear vibrations of cables in three dimensions, Part I: non-linear free vibrations, Journal of Sound and Vibration 118 (1987) 69–84.
[2] K. Takahashi, Y. Konishi, Nonlinear vibrations of cables in three dimensions, Part II: out-of-plane vibrations under in-plane sinusoidally time-varying load, Journal of Sound and Vibration 118 (1987) 85–97.
[3] F. Benedettini, G. Rega, Nonlinear dynamics of an elastic cable under planar excitations, International Journal of Nonlinear Mechanics 22 (1987) 497–509.
[4] G.V. Rao, R. Iyengar, Internal resonance and nonlinear response of a cable under a period excitation, Journal of Sound and Vibration 149 (1991) 25–41.
[5] K. Takahashi, Dynamic stability of cables subjected to an axial periodic load, Journal of Sound and Vibration 144 (1991) 323–330.
[6] N.C. Perkins, Modal interactions in the non-linear response of elastic cables under parametric/external excitation, Journal of Nonlinear Mechanics 27 (1992) 233–250.
[7] J.L. Lilien, A.P. Pinto da costa, Vibration amplitudes caused by parametric excitation on cable stayed structures, Journal of Sound and Vibration 174 (1994) 69–90.
[8] Y. Fujino, H. Oshima, P. Phoonsak, H. Yamaguchi, In-plane nonlinear vibrations of a cable and ergodic problem of their modes, Proceedings of the 43rd Annual Conference of the Japan Society of Civil Engineers, 1988, pp. 882–883 (in Japanese).
[9] J.A. Bennett, J.G. Eisley, A multiple-degree-of-freedom approach to nonlinear beam vibration, American Institute of Aeronautics and Astronautics Journal 8 (1970) 734–739.
[10] K. Takahashi, A method of stability analysis for nonlinear vibration of beams, Journal of Sound and Vibration 67 (1979) 43–54.
[11] H.M. Irvine, Cable Structures, The Massachusetts Institute of Technology Press, 1981.